



Supercapacitive Swing Adsorption of Carbon Dioxide**

Berenika Kokoszka, Nina K. Jarrah, Cong Liu, David T. Moore,* and Kai Landskron*

Abstract: An electrical effect, the supercapacitive swing adsorption (SSA) effect is reported, which allows for reversible adsorption and desorption of carbon dioxide by capacitive charge and discharge of electrically conducting porous carbon materials. The SSA effect can be observed when an electrically conducting, nanoporous carbon material is brought into contact with carbon dioxide gas and an aqueous electrolyte. Charging the supercapacitor electrodes initiates the spontaneous organization of electrolyte ions into an electric double layer at the surface of each porous electrode. The presence of this double layer leads to reversible, selective uptake and release of the CO_2 as the supercapacitor is charged and discharged.

The discovery of new electrical effects, such as the photovoltaic effect, superconductivity, or the thermoelectric effect, is a major driving force in science.^[1–3] The application of electrical potentials to matter allows for its manipulation, for example in liquid crystal displays as well as for electrically controlled hydrophobization and infiltration.^[4–6] Herein, we show that the charge and discharge of supercapacitor electrodes can be utilized to achieve gas adsorption and separation.

Monolithic, cylindrical carbon electrodes with a length of approximately 50 mm and a diameter of 13 mm (mass ca. 3.7 g) were prepared from commercially available activated carbon (BPL carbon, Calgon). One electrode was partially submerged, while the other electrode was fully submerged in 30 mL of an aqueous electrolyte (1M NaCl) inside a glass cell with a volume of 135 mL (Figure 1). The sorption cell was placed in a temperature-controlled water bath (299.00 ± 0.01 K) and flushed with a mixture of CO_2 and N_2 ($\text{CO}_2/\text{N}_2 = 15:85$) for four hours at atmospheric pressure. The chosen gas mixture resembles a mimic of flue gas. The system was sealed and equilibrated for twelve hours to allow for saturation of the electrolyte with the gas. After stabilizing the cell pressure for twelve hours, a potential difference of 1 V was applied using a Gamry 3000 potentiostat. The fully and partially submerged electrodes served as anode and cathode, respectively. The potentiostat enabled the coupling of the SSA experiments with whole-cell cyclovoltammetry (CV; scan rates: 1, 0.2, and 0.05 mV s^{-1}) and galvanostatic charge–

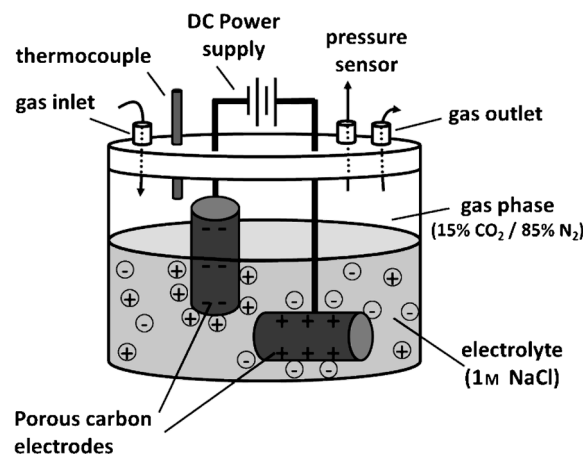


Figure 1. Experimental setup for an SSA experiment with aqueous electrolytes. Whereas the cathode is only partially submerged in the electrolyte, the anode is fully submerged.

discharge (GCD; current = 10 and 2 mA) experiments. The CV and GCD curves obtained confirmed the capacitive behavior of the system (Supporting Information, Figures S1–S5). With the GCD curves in hand, the capacitance C could be determined to be 57 F on average for all charge and discharge curves at 2 mA. The equivalent series resistance (ESR) that was measured from the current resistance (IR) drop was 17Ω . Reversible decreases (increases) in pressure that are associated with the charging (discharging) cycles were monitored during these experiments (Figure 2). However, there were significant differences in the pressure trends depending on whether a CV or a GCD scheme was employed and the specific parameters of the experiment. A pressure decrease was observed during the charge step of both the CV and the GCD experiments. The pressure increased by approximately the same value during the discharge step suggesting that the pressure changes are attributable to reversible adsorption of carbon dioxide. The magnitude of this supercapacitive swing adsorption (SSA) effect depended on the scan rate. For CV experiments, pressure changes of approximately 3, 9, and 17 Torr were observed (Figure 2a–c) for scan rates of 1, 0.2, and 0.05 mV s^{-1} , respectively. The pressure changes lag behind the applied voltage as the pressure minimum does not occur at the maximum voltage. This delay decreases with a decrease in the scan rate and is nearly absent for a scan rate of 0.05 mV s^{-1} . For the GCD experiments, reversible pressure changes of approximately 10 and 15 Torr were observed at 10 and 2 mA, respectively (Figure 2e, d). In this case, there is no delay for the pressure changes. The slope of the pressure curve (Figure 2d, e) that was obtained during the charging half cycle increases with time, which suggests that the magnitude of the SSA effect increases with the voltage. The

[*] B. Kokoszka, N. K. Jarrah, C. Liu, Prof. Dr. D. T. Moore, Prof. Dr. K. Landskron
Department of Chemistry, Lehigh University
6 East Packer Avenue (USA)
E-mail: david.moore@lehigh.edu
kal205@lehigh.edu

[**] The DOE ARPA is gratefully acknowledged for supporting this work (DE-AR-000026).

Supporting information for this article is available on the WWW under <http://dx.doi.org/10.1002/ange.201310308>.

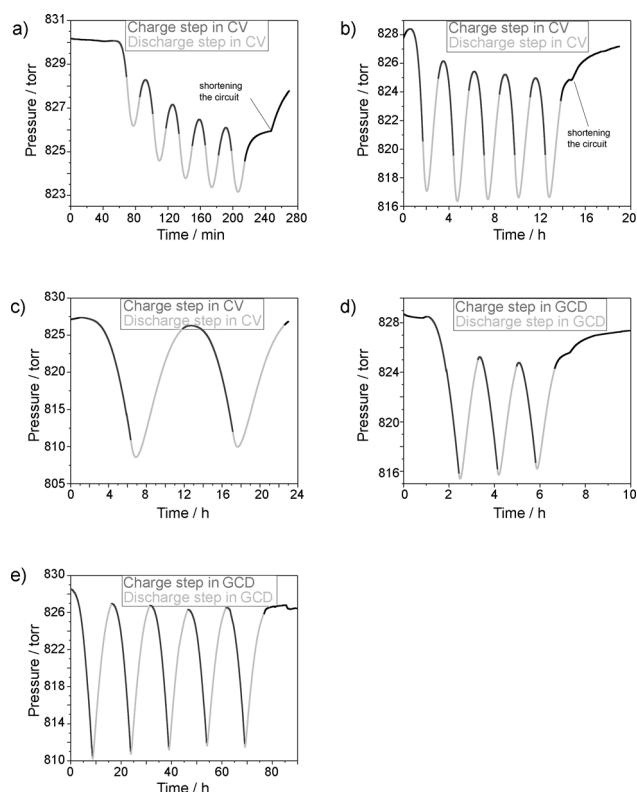


Figure 2. a–e) Pressure changes observed during cyclovoltammetric and galvanostatic charge (dark gray) and discharge (light gray) at 1 (a), 0.2 (b), and 0.05 mV s^{−1} (c), as well as at 10 (d) and 2 mA (e).

amount of energy that is required for charge and recovered by discharge may be calculated by multiplying the integration of the area under the GCD charge and discharge curves with the applied constant current (see the Supporting Information for details). At 10 mA, the energy that is required for charging is 22.2 J, and the energy that is recovered is 9.5 J, which corresponds to a charge–discharge energy efficiency of 42%. At 2 mA, the energy used for charging is 33.1 J; 24.4 J are recovered upon discharge, which is equivalent to a charge–discharge energy efficiency of 74%. This reflects the fact that the energy efficiency of a supercapacitor is a matter of the charge–discharge rate and the ESR of the capacitor.^[7,8] The smaller the ESR of a capacitor, the faster it can be charged at constant efficiency. The slower the charge rate, the higher the efficiency at constant ESR. The energy that is used per mol of reversibly adsorbed CO₂ in the experiment at 2 mA is 103.6 kJ mol^{−1} (see the Supporting Information for detailed calculations).

Reversible pressure changes were also observed when a conventional constant-voltage power supply was used as the voltage source. The pressure in the cell was continuously monitored while the potential difference across the electrodes was cycled between +1 V and 0 V (relative to ground), with the half-submerged and the fully submerged electrode assigned to be cathode and anode, respectively. The resulting pressure response for full cycles, which lasted 120 min each (one hour on and one hour off), is shown in Figure 3. These results clearly show a pressure response to the applied bias:

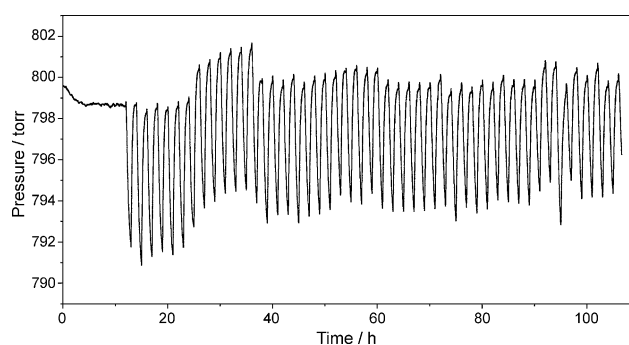


Figure 3. Pressure changes measured during the charge and discharge of electrodes with a constant-voltage power supply (1 V). During the charge step the pressure decreases. Electrode discharge leads to an increase in pressure.

The pressure decreases monotonically while the supercapacitor is charging (bias switched on), and then returns to its initial value (approximately) while the supercapacitor is discharging (bias off, electrodes short-circuited). This effect was reproducible over 50 charging/discharging cycles, with an average pressure swing of approximately 6 Torr.

The size of the pressure changes depends on the voltage. The pressure increased substantially from 3 Torr at 0.53 V to 31 Torr at 1.21 V for the first half cycle (Figure S6). The energy flow during voltage-dependent experiments was monitored using a power analyzer that was interfaced between the constant-voltage power supply and the electrodes; the values for the SSA effect are provided in Table S1. As the energy (E) that is stored in a capacitor is equal to $E = 0.5 CV^2$ (C = capacitance, V = voltage), we calculated the ratio $\Delta P/V^2$, which significantly increased from a value of 11.4 ($V = 0.53$ V) to 20.7 ($V = 1.21$ V). Similarly, the $\Delta P/E$ ratio increased from 0.87 to 1.71. The capacitive charging behavior of the system can be seen from the fact that E/V^2 is nearly constant. This suggests that greater pressure changes can be achieved at higher voltages. For a neutral aqueous electrolyte system, the maximum voltage is restricted to approximately 1.6 V, otherwise electrolysis takes place. From a thermodynamical point of view, the maximum voltage is restricted to approximately 1.2 V; however, approximately 1.6 V are possible practically in neutral solutions because of over-voltage effects.^[7]

Then, lighter and heavier electrodes were prepared, and the magnitude of the SSA effect was determined at a voltage of 1 V. Decreasing the mass of the electrode by a factor of 14 (0.2 g) decreased the magnitude of the pressure changes by a factor of approximately 14 (Figures S7 and S8). Increasing the mass of the electrodes to 7.5 g led to an approximate doubling of the magnitude of the effect. These results show that the effect scales linearly with the mass of the electrodes.

To assess the extent to which the observed SSA pressure changes reflected gas separation that is due to selective adsorption of CO₂ over N₂, the composition of the headspace gas was monitored by gas chromatography. Electrodes with masses of 7.5 g each were charged at a constant current of 2 mA between 0 and 1.2 V. Reversible pressure changes ranging from 47 Torr (first cycle) to 39 Torr (last cycle) were

measured (Figure S9). At the end of three half cycles, 10 μL aliquots of gas were sampled with a microliter syringe and the composition of the gas was analyzed by gas chromatography. At the end of an adsorption half cycle, the percentage of CO_2 in the gas mixture was reduced by between 6.5% and 5.5% (Table S2); this implies that more than one third of the carbon dioxide has been removed from the CO_2/N_2 (15:85) gas mixture. After completion of a desorption half cycle, the CO_2 content had increased by approximately the same extent (by between 6.1% and 5.4%). These results demonstrate that actual gas separation of CO_2 and N_2 from the mixture has taken place. The change in gas composition confirms that the observed pressure changes are due to selective adsorption of CO_2 from the gas mixture. A good agreement between the amount of reversibly adsorbed CO_2 that was calculated from the measured composition and the measured pressure changes further supports selectivity of CO_2 over N_2 (see the Supporting Information for details). The selectivity was confirmed by additional experiments with pure N_2 . The pressure slightly increased by approximately 0.5 Torr when a bias of 1 V was applied (Figure S10), which indicates that N_2 is slightly repelled from the supercapacitor. However, this very small effect may also be due to a more general phenomenon, such as the displacement of surface-adsorbed gas by electrowetting^[9] or even a density change of the electrolyte that is due to the formation of the double layer.

The dependence of the SSA effect on the partial pressure of CO_2 was also investigated. Experiments with pure CO_2 revealed an approximately four-fold increase in the effect compared to a 15:85 CO_2/N_2 mixture (Figure S11). As the partial pressure of CO_2 increased by a factor of 6.7 while the overall pressure changes only increased by a factor of 4, it may be concluded that there is a less than directly proportional dependence of the effect on the partial pressure of CO_2 .

The size of the effect for N_2/CO_2 gas mixtures as well as for pure CO_2 in thermodynamic equilibrium was investigated by extending the time of a single adsorption half cycle until no further decreases in pressure were observed. For the gas mixture, the effect was found to amount to approximately 55 and 70 Torr for a voltage of 1 and 1.2 V, respectively (Figure S12). For pure CO_2 , the effect was 97 Torr (1 V) and 109 Torr, respectively (Figure S13). The less than directly proportional relationship between the change in overall pressure and the change in the partial pressure of CO_2 is more strongly pronounced in systems at equilibrium, as the pressure only doubles while the CO_2 partial pressure increases from approximately 0.15 atm to approximately 1 atm. As the volume of the gas sorption cell and the mass of the electrodes are known, the magnitude of the effect could be calculated in terms of the amount of gas (in mol) per kilogram of carbon material to be 0.08 and 0.07 mol kg^{-1} for pure CO_2 at 1.2 and 1 V, respectively. In terms of the surface area, these values correspond to $1.2 \times 10^{-7} \text{ mol m}^{-2}$ and $1.1 \times 10^{-7} \text{ mol m}^{-2}$ (based on a $640 \text{ m}^2 \text{ g}^{-1}$ seven-point BET surface area for BPL carbon). For the gas mixture, the effect amounts to 0.04 mol kg^{-1} (1 V) and 0.05 mol kg^{-1} (1.2 V); these values correspond to 6.2×10^{-8} and $7.8 \times 10^{-8} \text{ mol m}^{-2}$, respectively.

Variable-temperature experiments with N_2/CO_2 gas mixtures in thermodynamic equilibrium revealed that the pres-

sure changes only weakly depend on the temperature (Figure S14). At 1.02 V, pressure changes of 55, 50, and 55 Torr were observed at temperatures of 26, 50, and 55 °C. At 1.2 V, the magnitude of the SSA effect increased to 67 Torr at 26 °C. At 40 and 55 °C, the pressure first decreased and then slowly increased. This phenomenon was more pronounced at 55 °C. Most likely, overvoltage effects, which prevent electrolysis at 1.2 V, are overcome at higher temperatures, which leads to the electrolytic evolution of gas. This hypothesis is further supported by the fact that the pressure at the end of an experiment is higher than at the beginning of the experiment. The observation that the pressure first decreases and then increases is due to the fact that at the beginning of an experiment, the pressure decrease that is due to the SSA effect is more pronounced than the pressure increase that arises from electrolysis. As the SSA effect saturates the pressure increase that is due to electrolysis becomes dominant.

Control experiments without any electrolyte at voltages of up to 5 kV did not show any pressure changes, which confirms that the electric double layer is essential for the SSA effect. In principle, the CO_2 could be adsorbed either at the gas–solid interface or at the electric double layer at the liquid–solid interface. Physisorption at a gas–solid interface is very fast and typically complete within seconds to minutes; however, the SSA effect requires several hours to reach equilibrium. This suggests that the adsorption takes place within the electrical double layer at the liquid–solid interface, because diffusion through a liquid is slower than diffusion through the gas phase. In this context, electrowetting, the wetting of a hydrophobic interface by the application of an electric bias,^[10] could play a significant role. It would be expected that the area of the reversibly wetted interface of the gas-exposed electrode increases (decreases) when the capacitor is charged (discharged). This also corroborates adsorption at the liquid–solid interface, as the magnitude of the pressure swings would then follow electrowetting-driven changes in the area of the liquid–solid interface, whereas they would be inversely correlated with changes at the gas–solid interface. To investigate which roles cathode and anode play we carried out an additional experiment, in which the half-exposed electrode acted as the anode, and the fully submerged electrode acted as the cathode. In this case, a reversible effect was also observed; however, the pressure somewhat increased when the electrodes were charged (Figure S15). This dependence on the polarity of the bias across the supercapacitor suggests that the SSA effect arises from the asymmetry between the interaction of CO_2 with the partially and fully submerged electrodes in the cell. Evidently, the CO_2 experiences a net stabilizing (destabilizing) interaction when the exposed electrode is biased as the cathode (anode); this indicates that the specific interactions of CO_2 with the cathode and anode must be different, presumably because of the different structures of the respective double layers. In a final control experiment, it was demonstrated that the SSA effect was still observed when an ionic liquid, namely tris(pentafluoroethyl)trifluorophosphate (EMIM FAP), was used as the electrolyte (Figure S16), which demonstrates that the effect is not limited to CO_2 in aqueous environments.

In conclusion, we have discovered a fundamentally new and non-obvious electrical effect, the supercapacitive swing adsorption effect, in which adsorption and desorption are accomplished by the reversible charge and discharge of supercapacitor electrodes. This SSA effect increases with applied voltage and demonstrates a high selectivity for CO₂ over N₂, enabling the separation of CO₂ from a mixture that mimics the composition of flue gas from a coal-fired power plant. The SSA effect decreases less than directly proportionally with the CO₂ partial pressure. The observed pressure changes are barely temperature-dependent. Aside from CO₂ separation, the SSA effect may also have implications for other gas separations as well as for gas storage, as the SSA effect may not be solely restricted to CO₂.

Received: November 27, 2013

Revised: December 23, 2013

Published online: February 24, 2014

Keywords: adsorption · carbon dioxide · porous carbon materials · separation · supercapacitors

- [1] D. Chiras, *Power from the sun*, New Society Publishers, **2009**, p. 39.
- [2] H. K. Onnes, *Proc. K. Ned. Akad. Wet.* **1911**, *13*, 1274.
- [3] P. Dai, B. C. Chakoumakos, G. F. Sun, K. W. Wong, Y. Xin, D. Lu, *Phys. C* **1995**, *243*, 201.
- [4] M. R. Powell, L. Cleary, M. Davenport, K. J. Shea, S. Z. Siwy, *Nat. Nanotechnol.* **2011**, *6*, 798.
- [5] D. Niu, J. Chen, W. Wang, Y. X. Wei, J. Hu, *Nucl. Sci. Technol.* **2011**, *22*, 240.
- [6] S. Kubo, Z.-Z. Gu, K. Takahashi, A. Fujishima, H. Segawa, O. Sato, *Chem. Mater.* **2005**, *17*, 2298.
- [7] Y. Cheng, *IEEE Trans. Energy Convers.* **2010**, *25*, 253.
- [8] Y. Zhong, J. Zhang, G. Li, A. Liu, *Internat. Conf. Power System Technol.* **2006**, *1*.
- [9] X. Yang, Y. He, G. Jiang, X. Liao, Z. Ma, *Electrochem. Commun.* **2011**, *13*, 1166.
- [10] W. Lu, T. Kim, A. Han, X. Chen, Y. Qiao, *J. Chem. Phys.* **2011**, *134*, 204706.